CYCLE TIME MODELS FOR AISLE CHANGING AS/RS CONSIDERING ACCELERATION/DECELERATION

Jörg Oser, Thomas Drobir
TU Graz, Austria

Abstract

In multi-aisle AS/RS systems one or more S/R machines serve several aisles with storage racks on both sides of the aisle. An important feature of multi-aisle configurations are aisle changing devices with transfer cars, curve guided aisle switching mechanisms or closed loop rail tracks with curved sections for a two-aisle layout.

These systems offer an economic solution, when the number of storage and retrieval transactions is low and storage volume is high. One or several S/R machines each serving a specified number of aisles can be arranged in various layouts to meet the required storage capacity and throughput.

1 Introduction and problem statement

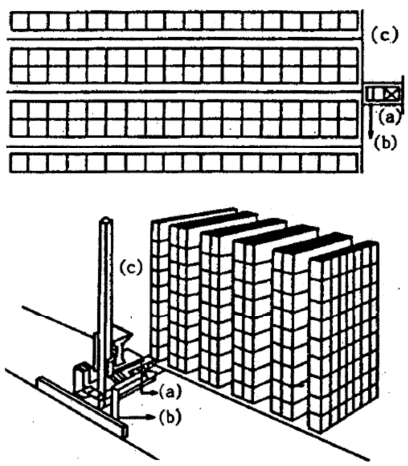

A long known aisle changing method consists of a transfer car also designated as traverser. It operates in an aisle perpendicular to the actual storage aisles. Figure 1 shows the arrangement of S/R machine riding on the traverser during the aisle changing operation.

The disadvantage of this solution is not only the additional costs of the traverser, but also a substantial loss in floor space and the extra waiting time when the S/R moves on and off the traverser.

Figure 1: S/R machine (a), traverser (b) [6]

A different option uses curve guided aisle switching mechanisms attached to the S/R machine.
Figure 2 from VDI 3658 shows how the aisle changing mechanism works with a tilting lever attached to a pair of guidance rollers.

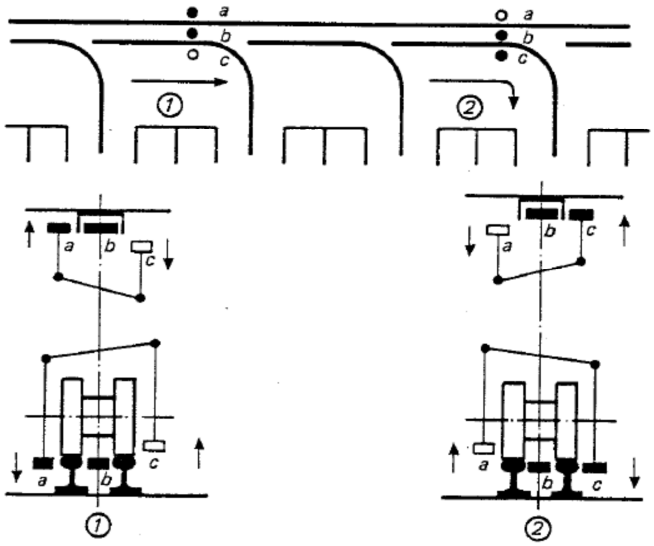

In position 1 the roller-pair a,b is meshing with the rail, so the S/R travels straight along the front aisle. Roller c is out of operation.

In position 2 the roller-pair b,c meshes with the rail curve section and diverts the S/R machine into the aisle requested by the PLC.

Figure 2: Aisle changing device with tilting lever mechanism. [11]

As can be seen the tilting lever can operate from below or above depending on the rail design. Due to the change of direction the curve speed has to be substantially lower than the nominal travel speed in straight motion.

As quite a few travel speed changes will occur during one cycle with two curve movements in single command (SC) and four such events in dual command (DC) operation with at least two start and two stop operations in SC, the influence of accelerations and decelerations for aisle changing S/R machines with curve switch devices for aisle changing will be significant.

A typical velocity-time-relationship for a one-leg SC cycle is shown in the following diagram. The graph shows six sections with different velocities necessary to approach a certain storage location. A typical feature is the reduced curve speed in section IV as well as the acceleration and de-celeration in sections I, III, V and VII.

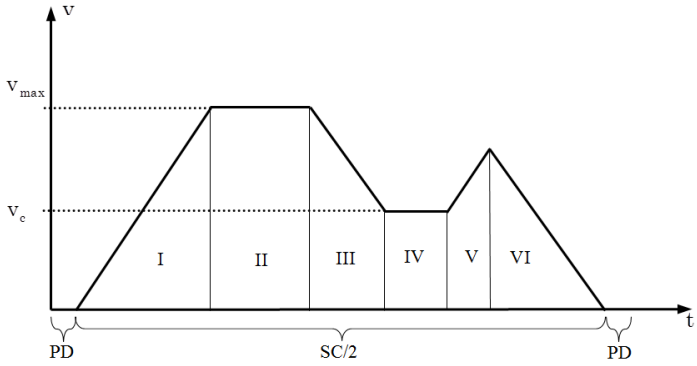

Figure 3: Velocity-time graph of curve travelling AS/RS

Thus this research aims at an improved cycle time calculation for multi-aisle AS/RS with curve travel considering acceleration/deceleration operating in SC and DC commands in a typical layout configuration.

The failure estimation not considering reduced curve speeds and accelerations, decelerations is investigated in figure 4.

The results show a 6-12% deviation for E(SC) and 10-16% for E(DC) operation. Thus, the reduced curve speed operation should not be neglected.

First Come First Serve (FCFS) is considered as the reference policy.

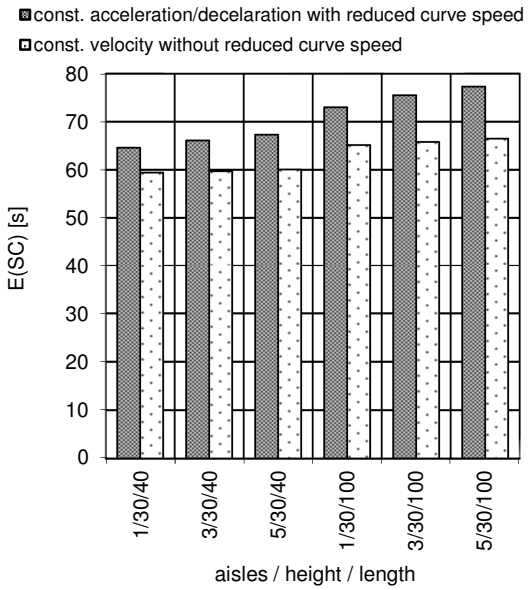

Figure 4:
E(SC) for different operations

The rest of the paper is organized as follows. In section 2 we present a literature review, in section 3 we derive the basic equations for various speed profiles leading to expressions for single and dual commands in section 4. In section 5 a comparative published example is used to verify our results. Finally, a number of case studies is treated by numerical evaluation in section 6 and a summary concludes our results in section 7.

2 Literature review

Roodbergen e.a. [1] present an extensive collection of research papers on AS/RS systems with a systematic approach showing that only very few papers deal with multi-aisle and operational issues. Early travel time models from Bozer e.a. [2] neglect acceleration and consider aisle captive systems only. Gudehus [3] includes acceleration in his model as early as 1973 but does not treat multi-aisle systems. His work was followed by Hwang e.a. [4] with an acceleration cycle time model also for aisle captive systems. Chang e.a. [5] approximates the cycle time by a polynomial expression and evaluates various theories with a piecewise variable velocity time function describing real world operating conditions, but his numerical results could not be verified. Hwang e.a. [6] develop a travel time model for multi-aisle application of transfer car aisle changing method. No acceleration effects or curve reduction speed are treated due to the transfer car method.

Benamar e.a. [7] treat the multi-aisle case using a visual Petri Net Developer also with a transfer car only and without modeling acc/dec effects. Egbelu [8] investigates the optimal dwell point location in a two aisle layout and suggests two linear programming optimization functions. However, Egbelu e.a. [9] revised the results from [8] with simulation results showing that empirical rules could outperform the optimization formulations. Hale e.a. [10] investigates the optimal dwell point location in multi-aisle AS/RS without considering acc/dec and aisle changing effects, which was done in [11].

3 Basic equations

In this chapter the speed profile of figure 3 describing a typical SC is separated into individual partitions as follows:

- Travel from IO to the beginning of the switching curve
- Travel within an aisle from the beginning of the switching curve
- Travel between aisles from curve to curve

For a trapezoidal speed profile for travel from IO to the beginning of the switching curve we obtain

$$s = \underbrace{\int_0^{\frac{v_{max}}{a}} a\,dt}_{\text{I}} + \underbrace{\int_{\frac{v_{max}}{a}}^{T-\frac{v_{max}-v_c}{a}} v_{max}\,dt}_{\text{II}} + \underbrace{\int_{T-\frac{v_{max}-v_c}{a}}^{T} a\left(T+\frac{v_c}{a}-t\right) dt}_{\text{III}} \tag{1}$$

according to figure 5.

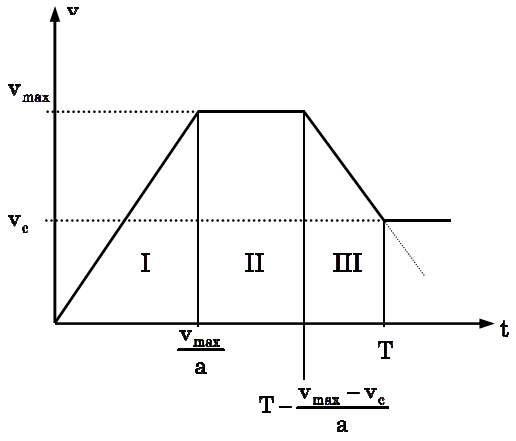

Figure 5: Trapezoidal travel from IO to curve

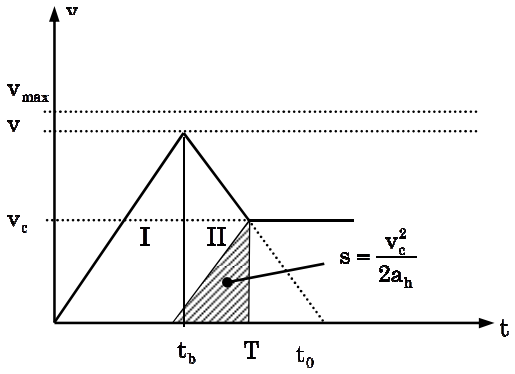

Figure 6: Triangular travel from IO to curve

Figure 5 becomes figure 6 with a triangular speed profile in case the minimum travel distance to the curve is $s_{min} = v_c^2/2a_h$ and v_{max} is not achieved.

The travel distance for figure 6 is shown in (2).

$$s = \underbrace{\int_0^{\frac{1}{2}(T+\frac{v_c}{a})} a\,dt}_{I} + \underbrace{\int_{\frac{1}{2}(T+\frac{v_c}{a})}^{T} a(T + \frac{v_c}{a} - t)\,dt}_{II} \tag{2}$$

Curve travel with reduced speed v_c results from figure 7.

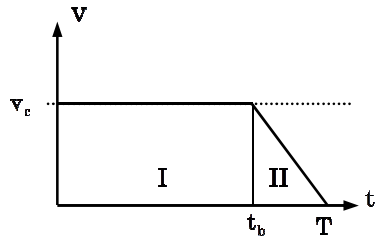

Figure 7: Curve speed profile for short travel distances

Travel distance s is

$$s = \underbrace{\int_0^{T-\frac{v_c}{a}} v_c\,dt}_{I} + \underbrace{\int_{T-\frac{v_c}{a}}^{T} a(T-t)\,dt}_{II} \tag{3}$$

The following speed profiles show the combination of curve travel with trapezoidal travel for long distances in figure 8 and for medium distances in figure 9 with triangular travel.

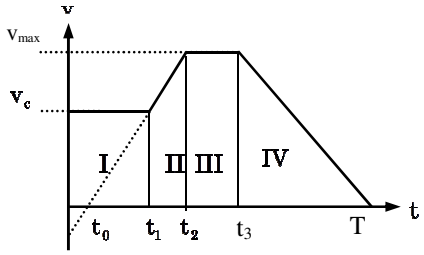

Figure 8: Long distance trapezoidal travel

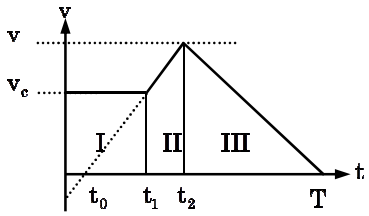

Figure 9: Medium distance triangular travel

The travel distance in figure 8 for trapezoidal travel is shown in (4) and for triangular travel according to figure 9 in (5).

$$s = \underbrace{\int_0^{\frac{l_c}{v_c}} v_c dt}_{\text{I}} + \underbrace{\int_{\frac{l_c}{v_c}}^{\frac{v_{max}-v_c}{a}+\frac{l_c}{v_c}} a\left(t - \frac{l_c}{v_c} + \frac{v_c}{a}\right) dt}_{\text{II}} + \underbrace{\int_{\frac{v_{max}-v_c}{a}+\frac{l_c}{v_c}}^{T-\frac{v_{max}}{a}} v_{max} dt}_{\text{III}} + \underbrace{\int_{T-\frac{v_{max}}{a}}^{T} a(T-t)\, dt}_{\text{IV}} \tag{4}$$

$$s = \underbrace{\int_0^{\frac{l_c}{v_c}} v_c dt}_{\text{I}} + \underbrace{\int_{\frac{l_c}{v_c}}^{\frac{1}{2}(T+\frac{l_c}{v_c}-\frac{v_c}{a})} a\left(t - \frac{l_c}{v_c} + \frac{v_c}{a}\right) dt}_{\text{II}} + \underbrace{\int_{\frac{1}{2}(T+\frac{l_c}{v_c}-\frac{v_c}{a})}^{T} a(T-t)\, dt}_{\text{III}} \tag{5}$$

The aisle changing cycle is defined by similar speed profiles as described in figures 5 and 6 in basic travel assuming a minimum curve speed of v_c.

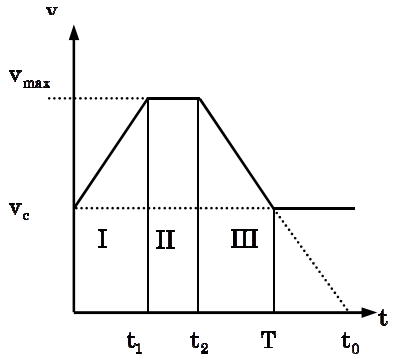

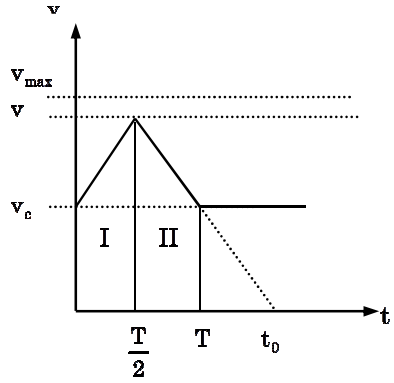

Figure 10: Aisle changing trapezoidal travel *Figure 11: Aisle changing triangular travel*

The referring travel distances for figure 10 and figure 11 are show in (6) for trapezoidal travel and in (7) for triangular travel.

$$s = \underbrace{\int_0^{\frac{v_{max}-v_c}{a}} (at + v_c) dt}_{\text{I}} + \underbrace{\int_{\frac{v_{max}-v_c}{a}}^{T-\frac{v_{max}-v_c}{a}} v dt}_{\text{II}} + \underbrace{\int_{T-\frac{v_{max}-v_c}{a}}^{T} a(T-t)\, dt}_{\text{III}} \tag{6}$$

$$s = \underbrace{\int_0^{\frac{T}{2}} (at + v_c) dt}_{\text{I}} + \underbrace{\int_{\frac{T}{2}}^{T} (v_c - at)\, dt}_{\text{II}} \tag{7}$$

4 Single and dual commands

Single and dual commands require the definition of a basic layout. The simplest layout of the multi-aisle configuration is shown in Figure 12a and b.

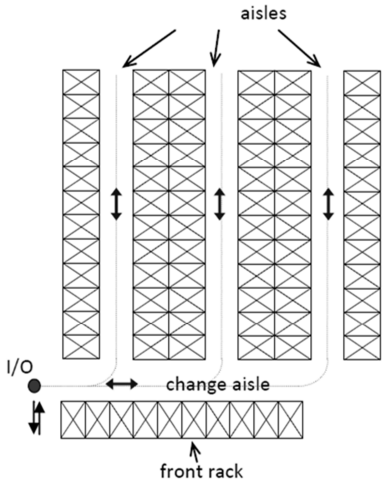

Figure 12a: Basic layout (Layout I)

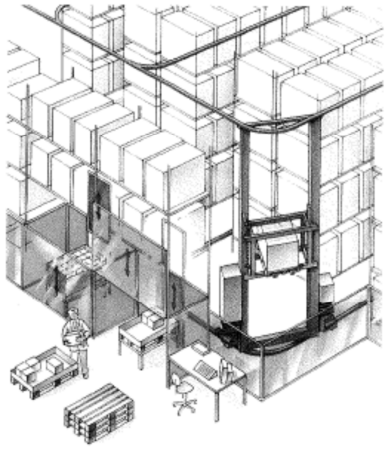

Figure 12b: AS/RS in curve travel [11]

Layout I assumes single and dual command operation with the dwell point at the I/O location, bidirectional travel of the S/R machine and reduced curve speed.

The results of further layouts are described as follows but the theory is not presented in this paper. Layout II has I/O stations at each end of a storage aisle opposite of the change aisle assuming bidirectional travel and SC/DC operation with the I/Os as dwell point policy. A third layout for higher throughput requirements is a closed loop system with several S/R machines, unidirectional travel and only one I/O.

Layout II is also used in industry, whereas Layout I is considered as a basic reference layout. Further basic assumptions are:

- Continuous rectangular storage rack with randomized storage assignment
- I/O point in variable positions depending on the layout
- Technical data of S/R machine (speeds, accelerations etc) and rack size
- Simultaneous S/R machine travel in horizontal and vertical directions
- Both triangular and trapezoidal velocity time functions may occur
- The full curve velocity v_c is always achieved

According to these assumptions, the formulas for SC and DC are derived.

The first partial travel time from IO to curve start follows from equations (1) and (2) with boundary conditions including the curve speed v_c.

$$t_{l_j}(s)=\begin{cases}\dfrac{1}{a_h}\sqrt{4sa_h+2v_c^2}-\dfrac{v_c}{a_h} & \text{für } 0<s\le\dfrac{2v_h-v_c}{a_h}\\ \dfrac{s}{v_h}+\dfrac{v_h-v_c}{a_h}-\dfrac{v_c^2}{2a_hv_h} & \text{für } \dfrac{2v_h-v_c}{a_h}<s\le l_j\end{cases} \tag{8}$$

The second partial travel time from the start of the curve to the storage location in SC follows from

$$t_{c_j}(s)=\begin{cases}\dfrac{s}{v_c}+\dfrac{v_c}{2a_h} & l_c<s\le\psi_1\\ \dfrac{l_c}{v_c}-\dfrac{v_c}{a_h}+\dfrac{1}{a_h}\sqrt{4(s-l_c)a_h+2v_c^2} & \text{für } \psi_1<s\le\psi_2\\ \dfrac{(s-l_c)}{v_h}+\dfrac{v_h-v_c}{a_h}+\dfrac{v_c^2}{2a_hv_h}+\dfrac{l_c}{v_c} & \psi_2<s\le l_c+L_j\end{cases} \tag{9}$$

with boundary conditions $\psi_1=l_c+\dfrac{v_c^2}{2a_h}$ and $\psi_2=l_c+\dfrac{v_h^2}{a_h}-\dfrac{v_c^2}{2a_h}$

Calculating the distance functions from the first partial travel time defined in (8) leads to equation (10)

$$s_{l_j}(t)=\begin{cases}\dfrac{a_h}{4}t^2+\dfrac{v_c}{2}t-\dfrac{v_c^2}{4a_h} & \text{für } 0<t\le\xi_0\\ v_ht-2\dfrac{v_h}{a_h}+\dfrac{v_c^2}{2a_h} & \text{für } \xi_0<t\le T_{l_j}\end{cases} \quad \text{with} \quad \xi_0=\frac{v_h^2}{a_h}-\frac{v_c^2}{2a_h} \quad \text{and} \quad T_{l_j}=\frac{l_j}{v_h}+\frac{v_h-v_c}{a_h}-\frac{v_c^2}{2a_hv_h} \tag{10}$$

Calculating the distance functions from the second partial travel time (9) leads to equation (11)

$$s_j(t)=\begin{cases}v_ct-\dfrac{v_c^2}{2a_h} & \text{für } \xi_0\le t\le\xi_1\\ \dfrac{a_h}{4}t^2+(\dfrac{v_c}{2}-\dfrac{a_hl_c}{2v_c})t+\dfrac{l_c^2a_h}{4v_c^2}+\dfrac{l_c}{2}-\dfrac{v_c^2}{4a_h} & \text{für } \xi_1<t\le\xi_2\\ v_ht+\dfrac{v_cv_h}{a_h}-\dfrac{v_c^2}{2a_h}-\dfrac{v_h^2}{a_h}+l_c(1-\dfrac{v_h}{v_c}) & \text{für } \xi_2<t\le T_{c_j}\end{cases} \tag{11}$$

with boundary conditions $\xi_0=\dfrac{l_c}{v_c}+\dfrac{v_c}{2a_h}$, $\xi_1=\dfrac{l_c}{v_c}+\dfrac{v_c}{a_h}$ and $\xi_2=\dfrac{l_c}{v_c}+\dfrac{2v_h-v_c}{a_h}$

The probability-density-function (pdf) is derived from the following transformation

$$dF_h(z) = f_h(z)dz = \frac{ds}{s_{max}} \quad \rightarrow \quad f_h(z) = \frac{1}{s_{max}}\frac{ds}{dz} \tag{12}$$

Therefore, the transformation result for the horizontal travel time to the j^{th} aisle is

$$f_{h_j}(z) = \frac{1}{L_j}\begin{cases} v_c & \xi_0 + t_{l_j} \le z \le \xi_1 + t_{l_j} \\ \frac{a_h}{2}(z - t_{l_j}) + \frac{v_c}{2} - \frac{a_h l_c}{2v_c} \text{ für } & \xi_1 + t_{l_j} < z \le \xi_2 + t_{l_j} \\ v_h & \xi_2 + t_{l_j} < z \le T_{j_{max}} \end{cases} \tag{13}$$

with boundary conditions $\xi_0 = \frac{l_c}{v_c} + \frac{v_c}{2a_h}$, $\xi_1 = \frac{l_c}{v_c} + \frac{v_c}{a_h}$, $\xi_2 = \frac{l_c}{v_c} + \frac{2v_h - v_c}{a_h}$ and $T_{j_{max}} = t_{l_j}(s = l_j) + T_{c_j}$

In order to derive the total horizontal travel-time pdf the f_{hj} has to be weighted with the number n_j of storage locations within the region j.

$$f_h(z) = \frac{1}{n_{ges}}\sum_{j=1}^{J} n_j f_{h_j}(z) \quad \text{mit} \quad n_{ges} = \sum_{j=1}^{J} n_j \quad \text{fulfilling the standardizing condition} \quad \int_0^{+\infty} f_{h_j}(z)dz = 1 \tag{14}$$

Expressions for the vertical motion are derived in a similar manner considering three different cases.

- Case 1: IO-location at zero level and immediate vertical motion
- Case 2: IO-location at zero level and delayed vertical motion
- Case 3: IO-location at random height

The total cumulative-density-function (cdf) for the j^{th} aisle follows from the product of horizontal h and vertical v distributions.

$$G_j(z) = F_{h_j}(z) \cdot F_v(z) \tag{15}$$

Evaluating an AS/RS with J aisle leads (15) to

$$G(z) = \frac{1}{J}\sum_{j=1}^{J} G_j(z) = \frac{1}{J}\sum_{j=1}^{J} F_{h_j}(z) \cdot F_v(z) \tag{16}$$

These equations finally result in the expected value for SC operation from

$$E(SC) = 2\int_0^{\infty} [1 - G(z)]dz \tag{17}$$

In a similar procedure the equations of dual command cycles are developed based on figure 13 but due to lengthy expressions they are not exhibited here.

SC_1	SC travel from IO to storage location (SL)
TB	time between SL and retrieval location (RL)
SC_2	single-command travel from RL to IO
PD	Pick-up- and deposit-time
$c_{1\text{-}2}$,$c_{3\text{-}4}$	curve travel in first and second curve section

$$E(TB) = \frac{JE_j(TB) + 2\sum_{n=1}^{J-1}[(J-n)E_{|j-k|=n}(TB)]}{J + 2\sum_{n=1}^{J-1}(J-n)} \tag{18}$$

Equation 18 contains an approximate solution for E(TB) based on the weighted average of the expected values of the minimum and maximum travel times for an aisle change j-k.

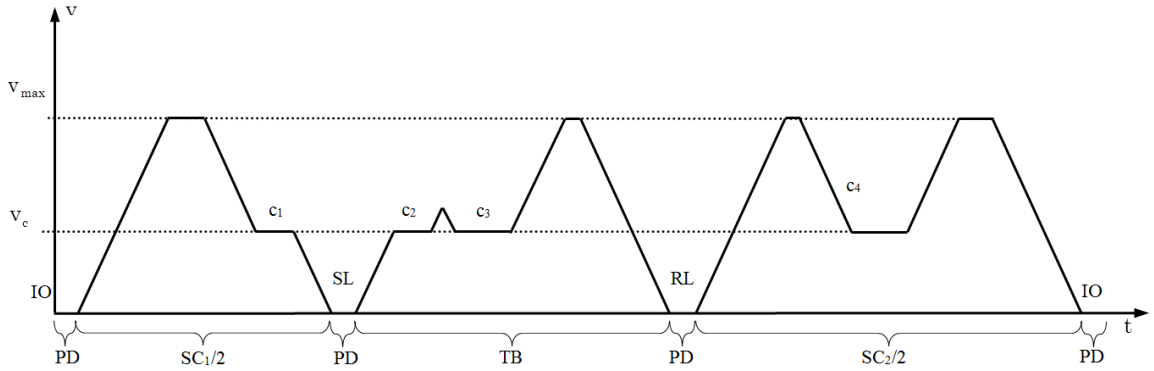

Figure 13: Speed profile for DC operation

5 Verification with literature results

We have verified our results with an analytical literature example from HWANG/KO [6] and with discrete event simulation using AutoMod™ and complete enumeration.

HWANG/KO investigated a case study according to figure 1 with the following basic differences to our research

- The time to transfer the S/R machine results from a discontinuous operation of the traverser mechanism, whereas we assume continuous aisle changing mechanisms with reduced curve speed.

- Acceleration and deceleration is assumed to be instantaneous whereas we assume limited values from drive characteristics.

AS/RS data are defined by

- Horizontal travel v_h=356 ft/min = 1,808 m/s
- Vertical travel v_v=100 ft/min = 0,508 m/s
- Transfer speed v_t= 50 ft/min = 0,254 m/s
- Rack length L=348 ft = 106 m
- Rack height H= 88 ft = 27 m

Furthermore, we simplified our calculations according to the assumptions stated above to make HWANG/KO's results comparable to our theory with

- Infinite horizontal acceleration
- Infinite vertical acceleration
- Curve radius R=0
- Curve speed equals horizontal speed v_c=v_h

Numerical evaluation of our theory in chapter 4 leads to the following results

# Aisles	E(SC) HWANG/KO	E(SC) DROBIR	E(DC) HWANG/KO	E(DC) DROBIR
1	1,2416 min	1,2420 min	1,6757 min	1,6710 min
2	1,4435 min	1,4394 min	2,2984 min	2,2196 min
3	1,6849 min	1,6778 min	2,7370 min	2,6398 min
4	1,9509 min	1,9419 min	3,1841 min	3,0438 min
5	2,2285 min	2,2185 min	3,6096 min	3,4736 min

Table 1: Comparison of SC and DC, [6] and [11]

6 Numerical evaluation

6.1 SC operation of Layout I

In this section Layout I with five aisles, LxH=100x30m and three lifting cases are considered. Figures 14 to 16 show the cdf and pdf of one-leg travel time distributions for three cases.

The case studies have been conducted based upon the following values

- Horizontal travel v_h=3,0 m/s
- Vertical travel v_v=0,5 m/s
- Curve speed v_c=0,5 m/s
- Rack length L=100 m
- Rack height H= 30 m
- Horizontal acceleration a_h=0,5 m/s²
- Vertical acceleration a_v=0,5 m/s²
- No. of aisles J=5

The following one-leg probability- and cumulative-density-functions have been calculated based on the theory of chapter 4. One-leg means half of the total travel time of a SC cycle. Three different vertical operation assumptions were evaluated.

Case 1:
Figure 14 assumes the IO-point at the lower left corner location with E(SC)=2x38sec.=76sec. neglecting pick-up- and deposit-times but considering additional curve-speed time-losses.

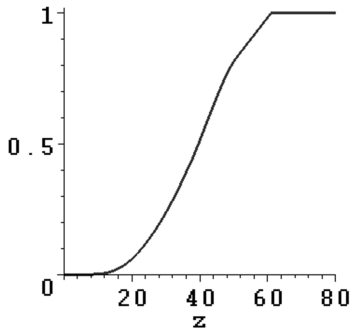

Figure 14a: Cdf of one-leg SC travel time

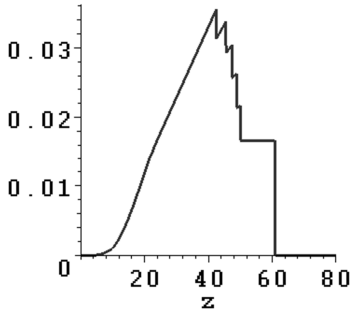

Figure 14b: Pdf of one-leg SC travel time

Case 2:
Figure 15 assumes the IO-point at the lower left corner location and a delayed lift operation starting at the end of the curve to minimize structure oscillation with E(SC)=2x41sec.=82sec. neglecting pick-up- and deposit-times but considering additional curve-speed time-losses.

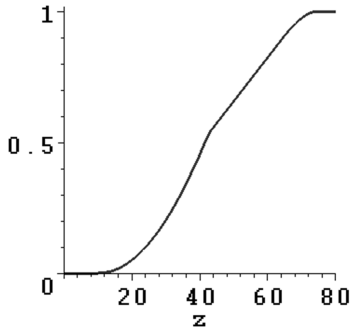

Figure 15a: Cdf of one-leg SC travel time

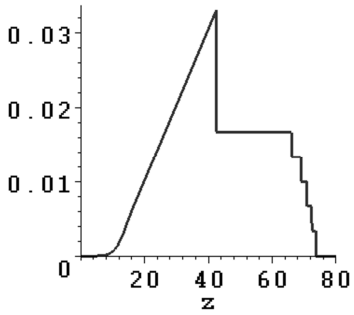

Figure 15b: Pdf of one-leg SC travel time

Case 3:
Figure 16 assumes the IO-point at half rack height H_{IO}=H/2 to minimize total cycle time with E(SC)=2x30,5sec.=61sec. neglecting pick-up- and deposit-times but considering additional curve-speed time-losses.

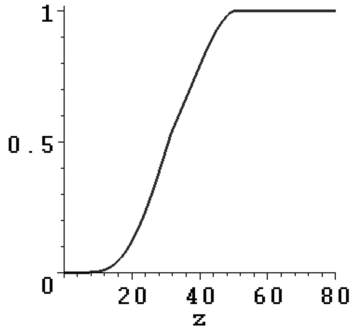

Figure 16a: Cdf of one-leg SC travel time

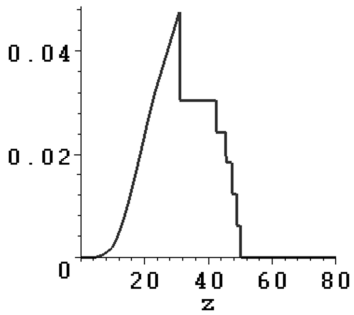

Figure 16b: Pdf of one-leg SC travel time

6.2 Comparative methods of calculating cycle times

First, a descrete event siumulation package (AutoMod™) was adopted to simulate AS/RS operation in multi-aisle layouts with simultaneous horizontal and vertical travel considering curve diverts and acceleration/deceleration.

A second method was to use Excel for averaging discrete cycle time calculation with complete enumeration of the relevant travel equations presented in section 4 for Layout I.

A third method was to use the analytical expressions derived in [11] for SC and DC operation presented here for E(SC) at the end of section 4.

Figure 17 exhibits the results of the expected value of SC operation E(SC) for Layout I with LxH=100x30m, varying the number of aisles from one to five and lifting case 1.

Figure 18 shows the expected values of dual command operation E(DC) again for Layout I with LxH=100x30m and lifting case 1.

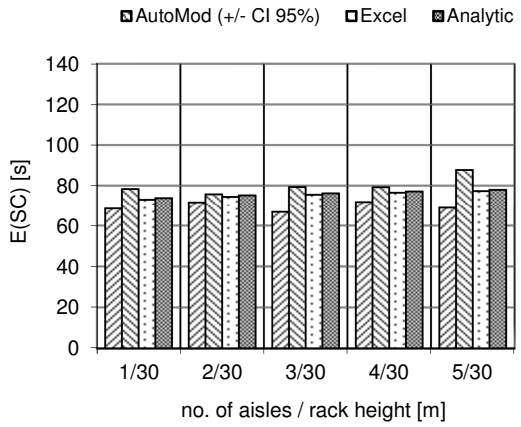

Figure 17: SC operation in Layout I

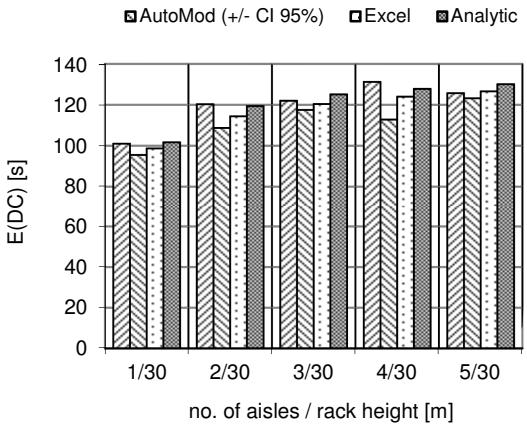

Figure 18: DC operation in Layout I

Two AutMod ™-results for each combination no. of aisles / rack height reflect the upper and lower bound of the 95% confidence interval of the simulation results.

Further results are shown in figure 19 for Layout II with LxH=100x30m and in figure 20 with the expected values of travel times E(DC) in dual command operation.

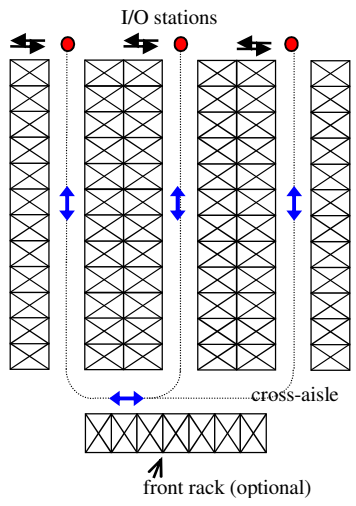

Figure 19: Layout II with multiple IO stations

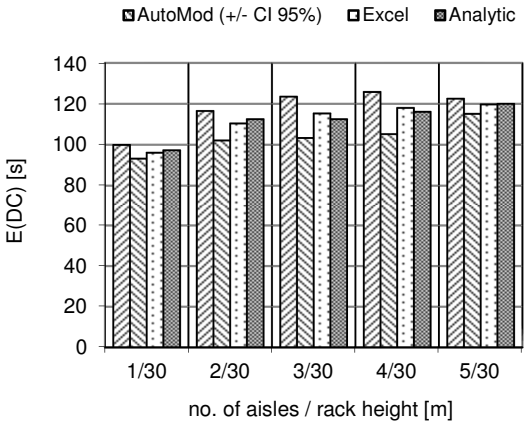

Figure 20: DC operation in Layout II

Layout II exhibits slightly smaller DC cycle times as compared to Layout I. Thus, multiple IO-stations in Layout II offer more throughput and flexibility of operations.

A third Layout III shows a unidirectional closed loop operation in figure 21 with LxH=100x30m and expected values for single command travel times E(SC) in figure 22.

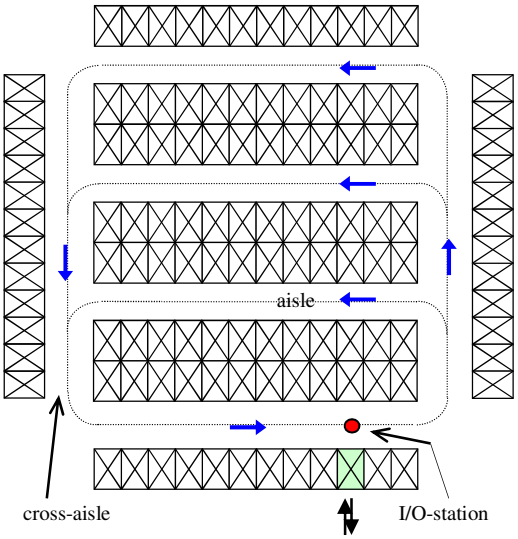

Figure 21: Unidirectional closed-loop Layout III

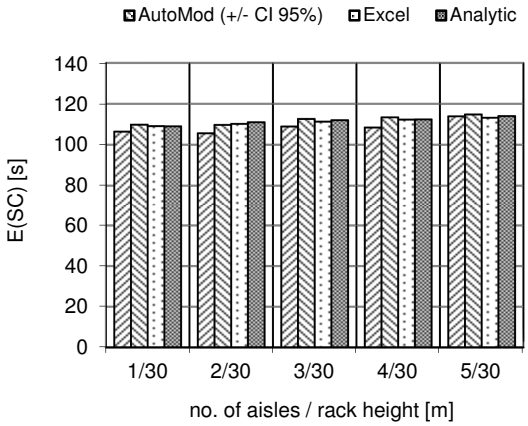

Figure 22: SC operation in Layout III

Comparing figures 22 and 17 shows for SC operation a throughput disadvantage of a closed loop Layout III compared to a bidirectional basic Layout I due to longer travel distances and more curves in closed loop systems.

Summary

First the basic velocity time relations are developed as algebraic expressions considering acceleration/deceleration with triangular and trapezoidal velocity-time functions when traveling with reduced curve velocities.
Assuming that a horizontal move consists of chronological superpositions of individual time sections further calculations of SC and DC operation are based on Tchebychev travel with the maximum of horizontal and vertical distance (time). These expressions are

later used to formulate the expected values in SC operation. They were verified and compared with simulation results and complete enumeration.
Applied to the selected layouts comparative results are obtained for different rack configurations. Numerical examples are presented and compared to literature results.

An extension of this research could include various dwell-point strategies and multiple AS/RS in multiple aisle configurations with one or several I/O-locations considering acceleration/deceleration and semi-continuous divert operation.

References

[1] Roodbergen, Kees Jan and Vis, F.A.Iris., "A survey of literature on automated storage and retrieval systems", *European Journal of Operational research* 194, 343-362 (2009)

[2] Bozer, Y.A. and White, J.A., "Travel time model for AS/RS systems", *IIE Transactions* 16 ,4, 329-338 (1984)

[3] Gudehus,T., *Grundlagen der Kommissioniertechnik,* Girardet Verlag (1973)

[4] Hwang, Hark and Lee, S.B., " Travel time models considering the operating characteristics of the storage and retrieval machine", *Int.Journal of Prod. Res.* 28,10,1779-1789(1990)

[5] Chang, D.T. and Wen, U.P. and Lin, J.T., "The impact of acceleration/deceleration on travel time models for automated storage/retrieval systems" *IIE Transactions* 27, 101-108 (1995)

[6] Hwang,Hark and Ko, C.S., "A study on multi-aisle system served by a single storage/retrieval machine" *Int.Journal of Prod. Res.* 26,11, 1727-1737 (1988)

[7] Benamar, A. and Sari,Z. and Ghouali, N., "Performance analysis for multi-aisle automated storage/retrieval systems using visual Petri Net developer", *Proc. 2003 IEEE Int. Symposium on Computational Intelligence in Robotics and Automation,* July 16-20, 2003, Kobe, Japan

[8] Egbelu, P., "Framework for dynamic positioning of storage/retrieval Machines in an automated storage /retrieval system *Int.Journal of Prod. Res.,* 29,1, 17-37 (1991)

[9] Egbelu, P. and Wu, C.T., "A comparison of dwell point rules in an Automated storage /retrieval system", *Int.Journal of Prod. Res.,*31,11, 2515-2530 (1993)

[10] Hale, Trevor S. and Hale, Leslie C., "Optimal dwell point locations in a multi-aisle AS/RS" *Proc. of the 7th Ind.Eng.Research Conference* Banff, Alberta, Canada, May 8-10 (1998)

[11] Drobir, T. "Spielzeitberechnung kurvengängiger Hochregallagersysteme", PhD Dissertation 2004, TU Graz